CrystEngComm

Accepted Manuscript

ROYAL SOCIETY OF CHEMISTRY

www.rsc.org/crystengcomm

Journal Name

RSCPublishing

COMMUNICATION

Two porous metal-organic frameworks containing zinc-calcium clusters or calcium cluster chains

Cite this: DOI: 10.1039/x0xx00000x

Kyungkyou Noh,[a] Nakeun Ko,[a] Hye Jeong Park,*[a] SangYoun Park*[b] and Jaheon Kim*[a]

Received 00th January 2012,
Accepted 00th January 2012

DOI: 10.1039/x0xx00000x

www.rsc.org/

A two-dimensional metal-organic framework (MOF) containing both Zn(II) and Ca(II) centres and a three-dimensional MOF containing only Ca(II) centres have the largest surface areas (BET 1560 and 914 m^2/g, respectively) among the reported Ca-based MOFs and also exhibit high gas uptakes up to 1 bar for H_2 at 77 K and CO_2 at 298 K.

The wide applicability of metal-organic frameworks (MOFs) for gas storage,[1] molecular separation,[2] catalysis,[3] sensing,[4] and biomedicine[5] is attributed to their tunable pore sizes, environments, and dynamics. A unique characteristic of MOFs is their high surface areas, which can be increased up to 7000 m^2/g;[6] almost a limit for porous materials. The surface areas, with consideration of pore volumes, can influence effective gas storage capability,[1] which has led to great research efforts being devoted to developing new synthetic strategies for highly porous MOFs. An example is the assembly of two or three different organic linkers together with well-defined inorganic secondary building units (SBUs). This proves to be a promising method, in combination with organic linker expansion, for developing highly porous MOFs as demonstrated in bio-MOFs 100-103,[7] UMCMs 1-5,[8] and MOF-177/200.[9] In contrast of the MOFs that have only one type of transition metal ions, an alternative strategy that combines common organic linkers with mixed metal or *s*- and *p*-block metal ions may be applicable to produce new porous structures. However, there is a high risk of unwanted structures that may be accompanied by inappropriate inorganic SBUs. Nevertheless, this direction is worth pursuing because there is a great possibility of achieving new MOF structural types.

Ca(II)-based MOFs have several benefits for applications in gas storage; the large abundance of Ca(II) sources in the earth (and thus its low cost) and the light weight of the Ca element are beneficial for making low-density and low-cost MOFs, which are important for practical gas storage application.[10-13] In addition, Ca-based MOFs are advantageous in bio-applications due to their nontoxicity and the biocompatibility of calcium ions.[14] Nonetheless, Ca(II)-based MOFs have yet to be satisfactorily explored, and those that are reported, rarely exhibit permanent porosity. There are difficulties in the design and prediction of proposed Ca-based MOFs because of the high coordination number and flexible coordination geometry of Ca(II).[15] Among the known Ca-based MOFs, two MOFs, CaSDB[10] and CaSBA,[11] are porous when evacuated; however, the BET surface areas are only 141 and 224 m^2/g, respectively. Among the mixed-metal MOFs that include the Ca(II) ion,[16] $[Zn_2Ca(BTC)_2(H_2O)_2]$ shows the highest BET surface area, 730 m^2/g.[12] These examples reflect the challenges experienced in synthesizing porous Ca-based MOFs having surface areas greater than 1000 m^2/g.

Common *s*- and *p*-block metal ions, Mg(II) and Al(III), prefer to form octahedral complexes, which limits the number of inorganic SBUs they can form during MOF synthesis. This is in contrast to transition metal ions that commonly have coordination numbers of 4 to 6. For Al(III) and Mg(II), the observed SBUs reported are fused octahedra as shown in MIL-53(Al)[17] or Mg-MOF-74.[18] Consequently, Ca(II) ions are expected to form different types of SBUs than those formed from transition metals, as mentioned above. Herein, we present two Ca(II)-based MOFs, ZnCaBTB and CaBTB formulated respectively as $[Zn_2Ca(BTB)_2(H_2O)_2]\cdot(THF)_{3.81}(H_2O)_{1.32}$ and $[Ca_5(BTB)_2(HBTB)_2(H_2O)_6]\cdot(THF)_{12}(H_2O)_2$, where BTB stands for benzene-1,3,5-tribenzoate, HBTB for mono-protonated BTB, and THF for tetrahydrofuran (Fig. 1). The crystal structures and gas adsorption properties of these MOFs are also presented.

Hexagonal-plate crystals of ZnCaBTB were obtained through a solvothermal reaction at 75 °C for 4 days, whereby both H_3BTB and $Zn(NO_3)_2\cdot6H_2O$ were first dissolved in a THF/H_2O solution and $Ca(OH)_2$ was subsequently added.

Rectangular-plate crystals of CaBTB were grown when a similar reaction mixture, without a Zn(II) source, was cooled at room temperature after heating the mixture at 85 °C for 7 days. The reaction conditions for CaBTB are unusual because most MOFs are produced during the heating rather than cooling process. Both MOF crystals are stable in common organic solvents, but become turbid or dissolve when exposed to air or water, respectively. Therefore, both MOFs were stored in THF prior to further analyses.

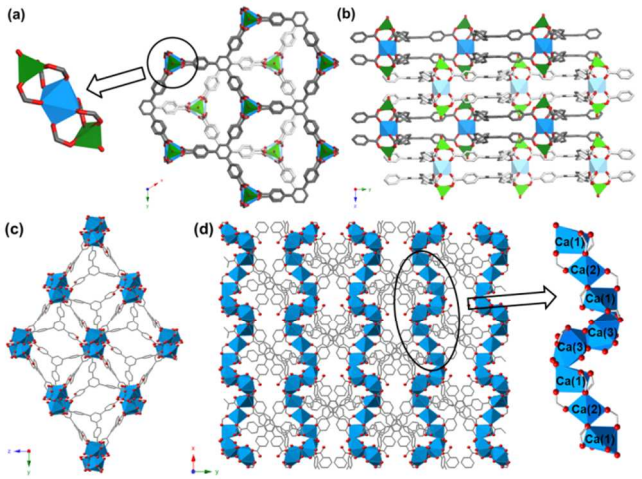

Fig. 1 Framework structures of (*a*, *b*) ZnCaBTB and (*c*, *d*) CaBTB with metal centres highlighted with polyhedrons. Colour codes: Zn, green; Ca, blue; C, grey; O, red. H atoms are omitted for simplicity. In (*a*), two alternative sheets are discerned with pale and deep colours.

The crystal structures of both ZnCaBTB and CaBTB were elucidated from the intensity data collected using a synchrotron light source. In ZnCaBTB, the inorganic SBU is a trigonal prism defined by six point-of-extension C atoms in a trinuclear cluster $Zn_2Ca(O_2C)_6$ (Fig. 1a). Every carboxylate group binds one Zn(II) and one Ca(II) ions in a bis-monodentate fashion. The terminal Zn(II) ions have a tetrahedral coordination geometry with four oxygen atoms from a water molecule and three carboxylate groups. The central Ca(II) is octahedrally coordinated by six carboxylate oxygen atoms. The identification of each metal ion was possible from X-ray structural refinement due to the large difference in electron densities. It is noted that almost the same cluster is found in $[Zn_2Ca(BTC)_2(H_2O)_2]$,[12] and similar clusters are also possible for Mg, Mn, Fe, Co, Ni, and Zn divalent ions. Therefore, it is reasonable to observe Ca(II) ions forming trinuclear clusters with these metal ions.

A stacked pair of two BTB linkers connect three inorganic SBUs to form two-dimensional (2D) honeycomb-like sheets running parallel to the crystallographic *ab* plane; that is, two BTBs together act as a 3-connector, and an inorganic SBU as also 3-connector. The diagonal distance of the resulting hexagon is 19.11 Å. Two central benzene rings in the BTBs are almost eclipsed when viewed along the *c*-axis with a centroid-to-centroid distance of 3.72 Å. Along the *c*-axis direction, a second sheet is stacked with 60° rotation in reference to the first sheet (Fig. 1a). This alternative (…ABAB…) stacking (Fig. 1b), with the separation of 3.65 Å, resembles the graphite structure and generates 1D channels with an effective window size of 3.8 Å (Figs. S2, S3). The void volume of ZnCaBTB is 44.4%, as estimated by PLATON.[19]

Compared with ZnCaBTB, CaBTB has a more complex three-dimensional (3D) structure (Fig. 1c). Three independent Ca(II) centres (Ca1, 2, and 3) in an asymmetric unit are expanded in lattice into trimer Ca_A (Ca1-Ca2-Ca1) and dimer Ca_B (Ca3-Ca3) clusters in a sequence of …Ca_A-Ca_B-Ca_A-Ca_B…., which forms an infinite inorganic SBUs roughly along the *a*-axis (Fig. 1d). Alternatively, the inorganic SBU can be described as a pentanuclear Ca_5 cluster composed of C_A and C_B that are repeatedly linked. (Crystallographic inversion centres are located at the centre of Ca_A and Ca_B.) The terminal oxygen atoms of BTB and HBTB are involved in five different coordination modes, as indicated in modes a to e in Scheme 1. Ca1 is 7-coordinated with six carboxylate oxygen atoms from two BTB (modes a and b) and two different HBTB linkers (modes a and c), and with one a water molecule. Ca2 is 6-coordinated with six carboxylate oxygen atoms from four BTB (mode b) and two HBTB linkers (mode c). Ca3 is 8-coordinated with five carboxylate oxygen atoms from two different BTB (modes a and d) and one HBTB linker (mode e), and with three water molecules. In short, a Ca_A-Ca_B cluster is bridged by ten carboxylate and two carboxylic acid groups, and coordinated by six coordinating water molecules to form a 3D framework with 3D curved channels (Fig. S7). The occluded six THF and one water molecules per asymmetric unit in the channels were identified in the crystal structure refinement, determining the chemical formula for CaBTB. The guest THF molecules are positioned to optimize the van der Waals contacts with themselves and the framework surfaces surrounded by the benzene rings of organic linkers (Fig. S8). Some of the THF molecules are also engaged in H-bonds with the coordinated (O1W, O2W, and O3W) and occluded (O4W) water molecules (Table S4). The void volume of CaBTB is 45.9%, as estimated by PLATON.[19] The powder X-ray diffraction (PXRD) pattern for the as-prepared CaBTB coincides well with the simulated pattern derived from the crystal structure (Fig. S9).

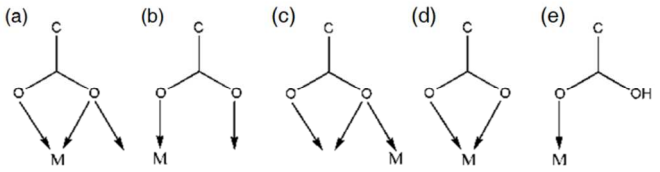

Scheme 1. Coordination modes of the carboxylate groups in CaBTB

The bulk phase purity of as-prepared ZnCaBTB was confirmed by comparison of the measured and simulated PXRD patterns (Fig. S10). The crystal structure revealed that THF and water molecules were occluded in the pore with partial site occupancy factors. Presumably due to the easy evaporation of solvent molecules, the elemental analysis gave a smaller

number of guest molecules: two THF and two H_2O per $Zn_2Ca(BTB)_2(H_2O)_2$. Thermogravimetric analysis (TGA) shows that ZnCaBTB lost 17.7% of mass at 200 °C presumably due to the evaporation of the occluded guest molecules (calcd. 21.6%) (Fig. S12). The final weight loss of organic linker was observed at 300 ~ 500 °C to afford metal oxides as the residue, which was determined, based on PXRD analysis, to be a mixture of hexagonal ZnO and cubic CaO (Fig. S11). A preliminary ICP-AES analysis of the dissolved ZnCaBTB crystals in an aqueous acidic solution indicated that the tentative molar ratio (Zn : Ca) was about 2.5 : 1. However, the crystal structure refinements on a series of structural models with various Zn/Ca ratios excluded any non-integer ratios of Zn/Ca (Table S1); each Zn and Ca must be located on a 3-fold axis and at a site with 32-symmetry, respectively, thus having a mole ratio of Zn/Ca = 2. A separate TGA analysis on the activated ZnCaBTB sample clearly shows that the framework is thermally stable up to 380 °C (Fig. S12).

TGA data for as-synthesized CaBTB (Fig. S13) reveals that guest molecules are removed at 200 °C (32.2%, calcd. 29.7%). The weight loss of organic linker exhibits two distinct steps at temperatures between 300 and 470 °C, suggesting the different thermal stabilities of BTB and HBTB. It is interesting that all organic parts are completely combusted at 560 °C to provide metal oxides as the remaining residue. A separate TGA analysis on the activated CaBTB sample indicates that the framework is thermally stable up to 350 °C.

The activated samples for ZnCaBTB and CaBTB were prepared by heating the as-prepared samples at 150 °C and 200 °C, respectively, for 6 h under vacuum. The PXRD measurements indicated that the framework structures of ZnCaBTB and CaBTB were maintained after the activation processes (Figs. S9, S10). Using the activated samples, the porosities of both MOFs were investigated. The N_2 gas sorption measurements for the two MOFs at 77 K show typical Type-1 sorption behaviours (Fig. 2a). The BET (Langmuir) surface areas of ZnCaBTB and CaBTB are 1560 (1970) and 914 (1170) m^2/g, respectively. To the best of our knowledge, the surface areas of ZnCaBTB and CaBTB are the highest among the data reported for Ca-based MOFs including both non-heterometallic and heterometallic Ca-MOFs.

In general, the pores or channels in non-interpenetrating 2D frameworks can hardly be developed and easily collapse upon removal of the guest molecules because the frameworks are founded upon weak interlayer interactions. Therefore, non-interpenetrating 2D MOFs exhibiting permanent porosity are rare.[20] In this regard; the permanent porosity of ZnCaBTB is an interesting result in combination with its high surface area. The extensive van der Waals interactions, which result in the 3.65 Å separation between the layers, appear to be retained during the activation process.

Interestingly, both ZnCaBTB and CaBTB uptake the same amount of H_2 gas (1.53 wt%) at 77 K and 1 bar (Figs. S14, and S15). This value is smaller than the 2.2 wt% observed for $[Zn_2Ca(BTC)_2(H_2O)_2]$, but is the second largest among the reported values for Ca-based MOFs.[10-13] For example, CaSDB[10] and CaSBA[11] displayed H_2 adsorption capacities of 0.55 wt% and 0.7 wt%, respectively under the same conditions. The CO_2 gas adsorption isotherms up to 1 bar collected at 253, 273, and 298 K indicate that ZnCaBTB can adsorb 266, 167, and 98 mg/g (Fig. S16) and CaBTB can store 246, 166, and 87 mg/g, respectively (Fig. S17). These capacities of ZnCaBTB and CaBTB at 298 K and 1 bar (Fig. 2b) are greater than any other Ca-based MOFs reported thus far.[10,11,13] The isosteric heats (Q_{st}) of CO_2 adsorption calculated by fitting the CO_2 adsorption isotherms at 253, 273, and 298 K to the virial equation indicate that the zero-coverage Q_{st} values of CO_2 adsorption in ZnCaBTB and CaBTB are 17.0 and 26.6 kJ/mol (Figs. S18 and S19), respectively, which are comparable to those of CaSDB (31 kJ/mol)[10] and CaSBA (28 kJ/mol).[11]

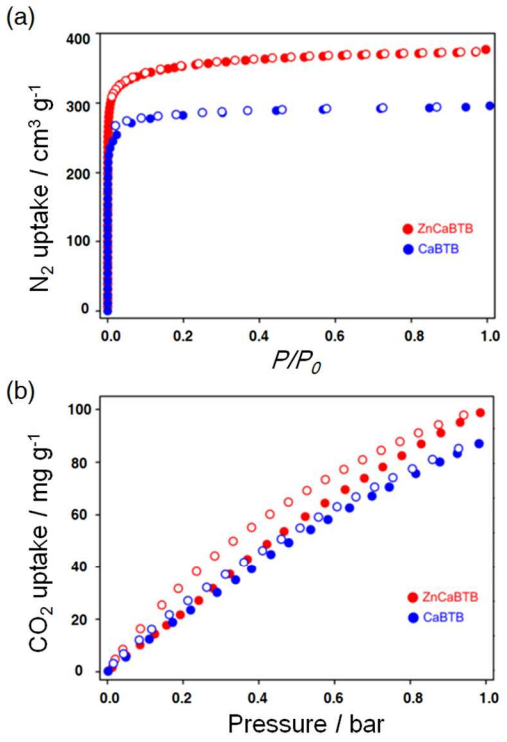

Fig. 2 Gas sorption isotherms for ZnCaBTB and CaBTB: (*a*) N_2 at 77 K and (*b*) CO_2 at 298 K.

In conclusion, we have prepared two porous Ca-based MOFs (ZnCaBTB and CaBTB) composed of trinuclear Zn_2Ca and pentanuclear Ca_5 clusters, respectively, linked by BTB units. The framework of ZnCaBTB has 2D layered structures generating 1D channels whereas CaBTB is a 3D framework with 3D curved channels. ZnCaBTB and CaBTB are unique examples for porous Ca-based MOFs. Additionally, ZnCaBTB is also a very rare example of a non-interpenetrating 2D MOF that displays permanent porosity. The surface areas and CO_2 uptake capacities at 298 K and 1 bar of ZnCaBTB and CaBTB are among the highest values reported thus far for any Ca-based MOFs (including non-heterometallic as well as heterometallic Ca-MOFs).

Acknowledgements

This research was supported by the Korea CCS R&D Center (KCRC) grant funded by the Korea government (Ministry of Science, ICT & Future Planning) (NRF-2012-0008900). Single-crystal X-ray diffraction data were collected using synchrotron radiation at a beamline 2D-SMC, Pohang Accelerator Laboratory (PAL) in Korea.

Notes and references

[a] *Institute for Integrative Basic Sciences, Department of Chemistry, Soongsil University, Seoul 156-743, Korea. Fax: +82 2 824 4383; Tel: +82 2 820 0459; E-mail: parkhyejeong83@gmail.com (H.J.P.), jaheon@ssu.ac.kr (J.K.)*
[b] *School of Systems Biomedical Science, Soongsil University, Seoul 156-743, Korea. Fax: +82 2 824 4383; Tel: +82 2 820 0459; E-mail: psy@ssu.ac.kr*

‡Electronic Supplementary Information (ESI) available: Experimental procedures, additional structure figures, TGA data, PXRD patterns, additional gas sorption data, and isosteric heats of CO_2 adsorption. CCDC 986349 (ZnCaBTB) and 986428 (CaBTB). See DOI: 10.1039/b000000x/

1 (*a*) M. P. Suh, H. J. Park, T. K. Prasad and D.-W. Lim, *Chem. Rev.*, 2012, **112**, 782; (*b*) K. Sumida, D. L. Rogow, J. A. Mason, T. M. McDonald, E. D. Bloch, Z. R. Herm, T.-H. Bae and J. R. Long, *Chem. Rev.*, 2012, **112**, 724; (*c*) T. A. Makal, J.-R. Li, W. Lua and H.-C. Zhou, *Chem. Soc. Rev.*, 2012, **41**, 7761.
2 J.-R. Li, J. Sculley and H.-C. Zhou, *Chem. Rev.*, 2012, **112**, 869.
3 C. Wang, D. Liu and W. Lin, *J. Am. Chem. Soc.*, 2013, **135**, 13222.
4 A. A. Talin, A. Centrone, A. C. Ford, M. E. Foster, V. Stavila, P. Haney, R. A. Kinney, V. Szalai, F. E. Gabaly, H. P. Yoon, F. Léonard and M. D. Allendorf, *Science*, 2014, **343**, 66.
5 A. C. McKinlay, R. E. Morris, P. Horcajada, G. Férey, R. Gref, P. Couvreur and C. Serre, *Angew. Chem. Int. Ed.*, 2010, **49**, 6260.
6 O. K. Farha, I. Eryazici, N. C. Jeong, B. G. Hauser, C. E. Wilmer, A. A. Sarjeant, R. Q. Snurr, S. T. Nguyen, A. Ö. Yazaydın and J. T. Hupp, *J. Am. Chem. Soc*., 2012, **134**, 15016.
7 T. Li, M. T. Kozlowski, E. A. Doud, M. N. Blakely and N. L. Rosi, *J. Am. Chem. Soc*., 2013, **135**, 11688.
8 K. Koh, A. G. Wong-Foy and A. J. Matzger, *J. Am. Chem. Soc*., 2010, **132**, 15005.
9 H. Furukawa, N. Ko, Y. B. Go, N. Aratani, S. B. Choi, E. Choi, A. O. Yazaydin, R. Q. Snurr, M. O'Keeffe, J. Kim and O. M. Yaghi, *Science*, 2010, **329**, 424.
10 (*a*) A. M. Plonka, D. Banerjee, W. R. Woerner, Z. Zhang, N. Nijem, Y. J. Chabal, J. Li and J. B. Parise, *Angew. Chem. Int. Ed.*, 2013, **52**, 1692; (*b*) D. Banerjee, Z. Zhang, A. M. Plonka, J. Li and J. B. Parise, *Cryst. Growth Des.*, 2012, **12**, 2162.
11 C.-T. Yeh, W.-C. Lin, S.-H. Lo, C.-C. Kao, C.-H. Lin and C.-C. Yang, *CrystEngComm*, 2012, **14**, 1219.
12 R. Zou, R. Zhong, S. Han, H. Xu, A. K. Burrell, N. Henson, J. L. Cape, D. D. Hickmott, T. V. Timofeeva, T. E. Larson and Y. Zhao, *J. Am. Chem. Soc.*, 2010, **132**, 17996.
13 (*a*) S. R. Miller, E. Alvarez, L. Fradcourt, T. Devic, S. Wuttke, P. S. Wheatley, N. Steunou, C. Bonhomme, C. Gervais, D. Laurencin, R. E. Morris, A. Vimont, M. Daturi, P. Horcajada and C. Serre, *Chem. Commun.*, 2013, **49**, 7773; (*b*) A. Mallick, E.-M. Schon, T. Panda, K. Sreenivas, D. Diaz Diaz and R. Banerjee, *J. Mater. Chem.*, 2012, **22**, 14951; (*c*) C. Borel, K. Davies, P. Handa, G. Hedberg, C. L. Oliver, S. A. Bourne, M. Hakansson, V. Langer and L. Ohrstrom, *Cryst. Growth Des.*, 2010, **10**, 1971; (*d*) S. Neogi, J. A. R. Navarro and P. K. Bharadwaj, *Cryst. Growth Des.*, 2008, **8**, 1554.
14 (*a*) W. Chen, W.-X. Chen, G. Zhuang, J. Zheng, L. Tan, X. Zhong and J. Wang, *CrystEngComm*, 2013, **15**, 5545; (*b*) A. Mantion, L. Massuger, P. Rabu, C. Palivan, L. B. McCusker and A. Taubert, *J. Am. Chem. Soc*., 2008, **130**, 2517.
15 (*a*) S Sheshmani, M. Ghadermazi, E Motieiyan, A. Shokrollahi, Z. Malekhosseini and M. A. Fashapoyeh, *J. Coord. Chem.*, 2013, **66**, 3949; (*b*) R. M. P. Colodrero, G. K. Angeli, M. Bazaga-Garcia, P. Olivera-Pastor, D. Villemin, E. R. Losilla, E. Q. Martos, G. B. Hix, M. A. G. Aranda, Ko. D. Demadis and A. Cabeza, *Inorg. Chem.*, 2013, **52**, 8770; (*c*) M. Mazaj, G. Mali, M. Rangus, E. Zunkovič, V. Kaučič and N. Z. Logar, *J. Phys. Chem. C*, 2013, **117**, 7552; (*d*) X. Liang, F. Zhang, W. Feng, X. Zou, C. Zhao, H. Na, C. Liu, F. Suna and G. Zhu, *Chem. Sci.*, 2013, **4**, 983; (*e*) X. Wang, L. K. San, H. Nguyen, N. M. Shafer, M. T. Hernandez and Z. Chen, *J. Coord. Chem.*, 2013, **66**, 826; (*f*) L. Han, L. Qin, L. Xu, Y. Zhou, J. Sun and X. Zou, *Chem. Commun.*, 2013, **49**, 406; (*g*) Y. Zhang, B. Guo, L.Li, S. Liu and G. Li, *Cryst. Growth Des.* 2013, **13**, 367; (*h*) A. Mallick, T. Kundu and R. Banerjee, *Chem. Commun.*, 2012, **48**, 8829; (*i*) A. M. Plonka, D. Banerjee and J. B. Parise, *Cryst. Growth Des.* 2012, **12**, 2460; (*j*) Z.-G. Gu, Y.-T. Liu, X.-J. Hong, Q.-G. Zhan, Z.-P. Zheng and S.-R. Zheng, W.-S. Li, S.-J. Hu and Y.-P. Cai, *Cryst. Growth Des.*, 2012, **12**, 2178; (*k*) N. Chen, J. Zhang, Y.-C. Gao, Z.-L. Yang, H.-J. Lu and G. Li, *J. Coord. Chem.*, 2011, **64**, 2554; (*l*) J. D. Furman, R. P. Burwood, M. Tang, A. A. Mikhailovsky and A. K. Cheetham, *J. Mater. Chem.*, 2011, **21**, 6595; (*m*) A. E. Platero-Prats, M. Iglesias, N. Snejko, A. Monge and E. Gutierrez-Puebla, *Cryst. Growth Des.* 2011, **11**, 1750; (*n*) M. K. Kim, K.-L. Bae and K. M. Ok, *Cryst. Growth Des.* 2011, **11**, 930; (*o*) P.-C. Liang, H.-K. Liu, C.-T. Yeh, C.-H. Lin and V. Zima, *Cryst. Growth Des.*, 2011, **11**, 699; (*p*) A. E. Platero-Prats, V. A. de la Pena-O'Shea, N. Snejko, A. Monge and E. Gutierrez-Puebla, *Chem. Eur. J.*, 2010, **16**, 11632; (*q*) D.-E Wang, F. Wang, X.-G. Meng, Y. Ding, L.-L. Wen, D.-F. Lia and S.-M. Lan, *Z. Anorg. Allg. Chem.*, 2008, **634**, 2643; (*r*) C. A. Williams, A. J. Blake, C. Wilson, P. Hubberstey and M. Schröder, *Cryst. Growth Des.*, 2008, **8**, 911; (*s*) K. Aliouane, N. Rahahlia, A. Guehria-Laidoudi, S. Dahaoui and C. Lecomte, *Acta Cryst.*, 2007, **E63**, m1834; (*t*) B. H. Hamilton, K. A. Kelly, W. Malasi and C. J. Ziegler, *Inorg. Chem.*, 2003, **42**, 3067; (*u*) D. T. de Lill, D. J. Bozzutoa and C. L. Cahill, *Dalton Trans.*, 2005, 2111.
16 (*a*) G.-L. Wen, M.-L. Han, F.-W. Wang, X. Zhao and C.-Y. Yin, *Z. Anorg. Allg. Chem.*, 2013, **639**, 2307; (*b*) K. Cui, F. Li, L. Xu, Y. Wang, Z. Suna and H. Fu, *CrystEngComm*, 2013, **15**, 4721; (*c*) L. Suescun, J. Wang, R. Faccio, G. Peinado, J. Torres, C. Kremer and R. A. Burrow, *Powder Diffr.*, 2012, **27**, 232; (*d*) J.-D. Lin, S.-T. Wu, Z.-H. Lia and S.-W. Du, *Dalton Trans.*, 2010, **39**, 10719; (*e*) E. Zhang, H. Hou, X. Meng, Y. Liu, Y. Liu and Y. Fan, *Cryst. Growth Des.*, 2009, **9**, 903.
17 T. Loiseau, C. Serre, C. Huguenard, G. Fink, F. Taulelle, M. Henry, T. Bataille and G. Férey, *Chem. Eur. J*., 2004, **10**, 1373.
18 S. R. Caskey, A. G. Wong-Foy and A. J. Matzger, *J. Am. Chem. Soc*., 2008, **130**, 10870.
19 A. L. Spek, *Acta Cryst*. 2009, **D65**, 148.
20 (*a*) W. J. Phang, W. R. Lee, K. Yoo, B.S. Kim and C. S. Hong, *Dalton Trans.*, 2013, **42**, 7850; (*b*) J. R. Karra, Y.-G. Huang and K. S. Walton, *Cryst. Growth Des.*, 2013, **13**, 1075; (*c*) A. Kondo, H. Kajiro, H. Noguchi, L. Carlucci,| D. M. Proserpio, G. Ciani, K. Kato, M. Takata, H. Seki, M. Sakamoto, Y. Hattori, F. Okino, K. Maeda, T. Ohba, K. Kaneko and H. Kanoh, *J. Am. Chem. Soc*., 2011, **133**, 10512; (*d*) L. Wen, P. Cheng and W. Lin, *Chem. Commun*., 2012, **48**, 2846; (*e*) K. L. Gurunatha and T. K. Maji, *Inorg. Chem.*, 2009, **48**, 10886 (*f*) S. Noro, D. Tanaka, H. Sakamoto, S. Shimomura, S. Kitagawa, S. Takeda, K. Uemura, H. Kita, T. Akutagawa and T. Nakamura, *Chem. Mater*., 2009, **21**, 3346; (*g*) C. B. Aakeroy, J. Desper and J. F. Urbina, *CrystEngComm,* 2005, **7**, 193.

Graphic Abstract

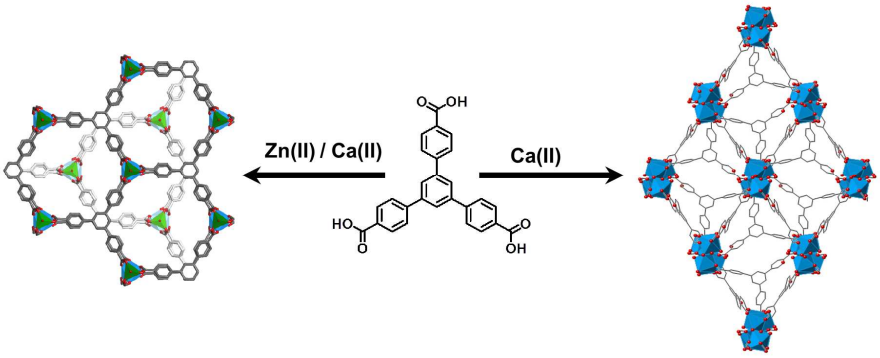

Two noble Ca-based metal-organic frameworks exhibit the largest surface areas and the highest CO_2 adsorption capacity at 298 K and 1 bar among the Ca-based MOFs reported so far.